THREE-DIMENSIONAL SIMULATION OF THERMAL OXIDATION AND THE INFLUENCE OF STRESS

Christian Hollauer, Hajdin Ceric, and Siegfried Selberherr
Institute for Microelectronics, Technical University Vienna
Gußhausstraße 27–29, A-1040 Wien, Austria

Abstract. The thermal oxidation process of three-dimensional structures is analyzed with our oxidation model. This comprehensive model takes into account that the diffusion of oxidants, the chemical reaction, and the volume increase occur simultaneously in a so-called reactive layer which has a spatial finite width, in contrast to the sharp interface between silicon and dioxide in the conventional formulation. Our oxidation model also includes the coupled stress dependence of the oxidation process because the influence of stress is shown to be considerable. Only the simulation of stress dependent oxidation leads to results which agree with the real physical behavior.

INTRODUCTION

Thermal oxidation of silicon is one of the most important steps in the fabrication of highly integrated electronic circuits, being mainly used for efficient isolation of adjacent devices from each other. If a surface of a silicon body has contact with an oxidizing atmosphere, the chemical reaction of oxidants with silicon (Si) forms silicon dioxide (SiO_2). Depending on the oxidizing ambient the oxidants can arise from steam (dry oxidation) or water vapour (wet oxidation). Wet oxidation has a significantly higher oxidation rate than the dry one and so wet oxidation is mainly applied for fast thick film oxidation in contrast to dry oxidation which is more suitable for thin film oxidation.

If a SiO_2 - domain already exists the oxidants diffuse through the SiO_2 - domain to the Si - SiO_2 - interface (1) where the chemical reaction of the oxidants with silicon takes place. The parts of silicon which should not be oxidized are masked by a layer of silicon nitride (Si_3Ni_4), because Si_3Ni_4 prevents the oxidant diffusion on the subjacent SiO_2 - layer. During the oxidation process the chemical reaction consumes Si and the newly formed SiO_2 has more than twice the volume of the original Si. This significant volume increase leads to large displacements in the materials.

If the additional volume is prevented from expanding as desired, e.g. by the Si_3Ni_4 - mask, mechanical stresses arise in the materials. Since there is a strong stress dependence of the oxidant diffusion and the chemical reaction, the oxidation process itself is considerably influenced by stress.

So thermal oxidation is a complex process where the three subprocesses oxidant diffusion, chemical reaction, and volume increase occur simultaneously. From a mathematical point of view the oxidation process can be described by a coupled system of partial differential equations, one for the diffusion of oxidants through SiO_2, the second for the conversion of Si into SiO_2 at the interface, and a third for the mechanical problem of the complete oxidized structure. The whole mathematical formulation is numerically solved by applying the finite element method.

The oxidation rate mainly depends on the oxidizing ambient, especially on the temperature, the pressure, and the oxidant species. For practical use of an oxidation model it is important to carefully control the ambient parameters of the oxidation process. Therefore in our model these parameters, e.g the temperature profile, are adjustable easily.

The Physics and Chemistry of SiO_2 and the $Si - SiO_2$ Interface – 5,
H. Z. Massoud, J. H. Stadhis, T. Hattori, D. Misra, and I. Baumvol, Editors,
ECS Transactions, Vol. 1, No. 1, The Electrochemical Society, Pennington, NJ, 2005.

(c) 2005 The Electrochemical Society

THE MODEL

In our oxidation model (2) we use a normalized silicon concentration $\eta(\vec{x},t)$ (3) so that the value of η is 1 in pure Si and 0 in pure SiO_2. Advantageously our model takes into account that the diffusion of oxidants, the chemical reaction and the volume increase occur simultaneously in a so-called reaction layer. In contrast to the sharp interface between Si and SiO_2 like in the standard model (4), this reaction layer has a spatial finite width (see Fig. 3) where the value of η lies between 0 and 1.

Most of the other oxidation models (5)(6) describe the SiO_2 - growth more or less by a moving boundary problem, because these models are all based on the one-dimensional standard model (4). Unfortunately the handling of moving boundary problems becomes very complicated for complex three-dimensional structures (7) and so sometimes such models are restricted to two dimensions or have a lack of reliability and stability for complex three-dimensional structures.

With regard to these aspects our oxidation model is advantageous, because with the normalized silicon concentration and the reaction layer it exhibits always the same reliability independent of the geometry of the three-dimensional structure. Furthermore all other oxidation models need a special fitting for thin film oxidation as described in (8). So another advantage of or model is that thin film or dry oxidation (9)(10) is also properly treated by our model without any modification.

Oxidant Diffusion

The diffusion of oxidants is described by

$$D(p)\,\Delta C(\vec{x},t) = k(\eta,p)\,C(\vec{x},t), \qquad [1]$$

where Δ is the Laplace operator, $C(\vec{x},t)$ is the oxidant concentration, and $D(p)$ is the stress dependent diffusion coefficient:

$$D(p) = D_0 \exp\left(-\frac{p\,V_D}{k_B\,T}\right). \qquad [2]$$

Here D_0 is the low stress diffusion coefficient (11)(12), p is the hydrostatic pressure in the respective material, V_D is the activation volume, k_B is the Boltzmann's constant, and T is the temperature in Kelvin.
$k(\eta,p)$ is the stress dependent strength of a spatial sink and not just a reaction coefficient at a sharp interface:

$$k(\eta,p) = \eta(\vec{x},t)\,k_{max} \exp\left(-\frac{p\,V_k}{k_B\,T}\right). \qquad [3]$$

As given in [3] we define that $k(\eta,p)$ is linearly proportional to $\eta(\vec{x},t)$. Furthermore [2] and [3] are only valid for a pressure $p \geq 0$.

Dynamics of η

The dynamics of η is described by

$$\frac{\partial\eta(\vec{x},t)}{\partial t} = -\frac{1}{\lambda} k(\eta,p)\,C(\vec{x},t)/N_1, \qquad [4]$$

where λ is the volume expansion factor ($=2.25$) for the reaction from Si to SiO_2, and N_1 is the number of oxidant molecules incorporated into one unit volume of SiO_2.

Mechanics

The chemical reaction of silicon and oxygen causes a significant volume increase. The normalized additional volume after time Δt is

$$V_{rel}^{add} = \frac{\lambda - 1}{\lambda} \Delta t \; k(\eta, p) C(\vec{x}, t)/N_1. \qquad [5]$$

The mechanical problem is described by the equilibrium relations

$$\begin{aligned} \frac{\partial \sigma_{xx}}{\partial x} + \frac{\partial \sigma_{xy}}{\partial y} + \frac{\partial \sigma_{xz}}{\partial z} &= 0 \\ \frac{\partial \sigma_{yx}}{\partial x} + \frac{\partial \sigma_{yy}}{\partial y} + \frac{\partial \sigma_{yz}}{\partial z} &= 0 \\ \frac{\partial \sigma_{zx}}{\partial x} + \frac{\partial \sigma_{zy}}{\partial y} + \frac{\partial \sigma_{zz}}{\partial z} &= 0 \end{aligned} \qquad [6]$$

where the stress tensor $\tilde{\sigma}$ is given by

$$\tilde{\sigma} = \mathbf{D}(\tilde{\varepsilon} - \tilde{\varepsilon_0}) + \tilde{\sigma_0}. \qquad [7]$$

Here $\mathbf{D}$ is the so-called material matrix. Furthermore, $\tilde{\varepsilon}$ is the strain tensor, $\tilde{\varepsilon_0}$ is the residual strain tensor, and $\tilde{\sigma_0}$ is the residual stress tensor.

The material matrix $\mathbf{D}$ can be splitted in a dilatation and a deviatoric part (13)

$$\mathbf{D} = \left(H \begin{bmatrix} 1 & 1 & 1 & 0 & 0 & 0 \\ 1 & 1 & 1 & 0 & 0 & 0 \\ 1 & 1 & 1 & 0 & 0 & 0 \\ 0 & 0 & 0 & 0 & 0 & 0 \\ 0 & 0 & 0 & 0 & 0 & 0 \\ 0 & 0 & 0 & 0 & 0 & 0 \end{bmatrix} + G_{eff} \begin{bmatrix} +\frac{4}{3} & -\frac{2}{3} & -\frac{2}{3} & 0 & 0 & 0 \\ -\frac{2}{3} & +\frac{4}{3} & -\frac{2}{3} & 0 & 0 & 0 \\ -\frac{2}{3} & -\frac{2}{3} & +\frac{4}{3} & 0 & 0 & 0 \\ 0 & 0 & 0 & 1 & 0 & 0 \\ 0 & 0 & 0 & 0 & 1 & 0 \\ 0 & 0 & 0 & 0 & 0 & 1 \end{bmatrix} \right) \qquad [8]$$

with the bulk modulus H and the effective shear modulus G_{eff}. The bulk modulus is

$$H = \frac{E}{3(1 - 2\nu)}, \qquad [9]$$

where E is the Young modulus and ν is the Poisson ratio.

In the elastic case G_{eff} is the same as the standard shear modulus

$$G_{eff} = G = \frac{E}{2(1 + \nu)}. \qquad [10]$$

The materials SiO_2 and Si_3Ni_4 have a viscoelastic behavior (14). The Maxwellian formulation of viscoelasticity is the most suitable one for these materials (15). In Maxwell's model the dilatation part is assumed purely elastic while the deviatoric part is modelled by a Maxwell element.

It can be assumed that for a short time period ΔT the strain velocity can be kept constant ($\dot{\varepsilon} = \frac{\varepsilon}{\Delta T}$) (16). So in the viscoelastic case G_{eff} can be written in the form

$$G_{eff} = G \frac{\tau}{\Delta T} \Big(1 - \exp\big(- \tfrac{\Delta T}{\tau} \big) \Big), \qquad [11]$$

where τ is the Maxwellian relaxation time. This relationship shows that Maxwell viscoelasticity can be expressed by an effective rigidity G_{eff} in the deviatoric part of [8]. So the material matrix

(c) 2005 The Electrochemical Society

$\mathbf{D}$ depends in the elastic case only on Young's modulus E and the Poisson ratio ν, and in the viscoelastic case additionally on the Maxwellian relaxation time τ.

The components $\varepsilon_{0,ii}$ (i stands for x, y or z) of the residual strain tensor $\tilde{\varepsilon_0}$ are linear proportional to the normalized additional volume from

$$\varepsilon_{0,ii} = \tfrac{1}{3} V_{rel}^{add}. \qquad [12]$$

After discretization of the continuum, we obtain a linear equation system for the mechanical problem

$$\mathbf{K}\vec{d} = \vec{f} \quad \text{with} \quad \mathbf{K} = \int_{\mathcal{V}} \mathbf{B^T D B} dV, \qquad [13]$$

where $\mathbf{K}$ is the so-called stiffness matrix, $\vec{d}$ is the displacement vector, and $\vec{f}$ is the force vector.

$$\mathbf{B} = [\mathbf{B_i}, \mathbf{B_j}, \mathbf{B_m}, \mathbf{B_p}] \qquad [14]$$

is a discretized partial derivative matrix (17) where i, j, m and p are the four nodes on a single tetrahedral element. The submatrix $\mathbf{B_i}$ for the node i is

$$\mathbf{B_i} = \begin{bmatrix} \frac{\partial N_i}{\partial x} & 0 & 0 \\ 0 & \frac{\partial N_i}{\partial y} & 0 \\ 0 & 0 & \frac{\partial N_i}{\partial z} \\ \frac{\partial N_i}{\partial y} & \frac{\partial N_i}{\partial x} & 0 \\ 0 & \frac{\partial N_i}{\partial z} & \frac{\partial N_i}{\partial y} \\ \frac{\partial N_i}{\partial z} & 0 & \frac{\partial N_i}{\partial x} \end{bmatrix} = \begin{bmatrix} b_i & 0 & 0 \\ 0 & c_i & 0 \\ 0 & 0 & d_i \\ c_i & b_i & 0 \\ 0 & d_i & c_i \\ d_i & 0 & b_i \end{bmatrix}, \qquad [15]$$

with the linear form function $N_i(\vec{x})$ defined as

$$N_i(\vec{x}) = a_i + b_i\, x + c_i\, y + d_i\, z, \qquad [16]$$

in which a_i, b_i, c_i and d_i are constant geometrical coefficients for the finite element. For example b_i is

$$b_i = -\det \begin{vmatrix} 1, & y_j, & z_j \\ 1, & y_m, & z_m \\ 1, & y_p, & z_p \end{vmatrix}. \qquad [17]$$

The force vector on a finite element depends on the residual strain tensor and thus also on the volume increase

$$\vec{f} = \int_{\mathcal{V}} \mathbf{B^T D} \tilde{\varepsilon}_0\, dV. \qquad [18]$$

After solving the linear equation system [13] we obtain the displacement vector. Since the strain is the first derivative with respect to displacement

$$\tilde{\varepsilon} = \mathbf{B}\vec{d}, \qquad [19]$$

the stress can be determined with equation [7].

With the stress tensor the pressure for [2] and [3] can be determined by using the formula

$$p = -\frac{\text{Trace}(\tilde{\sigma})}{3} = -\frac{\sigma_{xx} + \sigma_{yy} + \sigma_{zz}}{3}. \qquad [20]$$

(c) 2005 The Electrochemical Society

SIMULATION PROCEDURE

For the simulation procedure we perform a finite element discretization by splitting the three-dimensional structure into tetrahedral elements. The size of the tetrahedrons and, as a result of that, the number of finite elements is controlled adaptively by a meshing module. In the next step we set the initial values for the oxidant concentration C and the normalized silicon concentration η on the grid nodes. For example η must be 1 in pure Si.

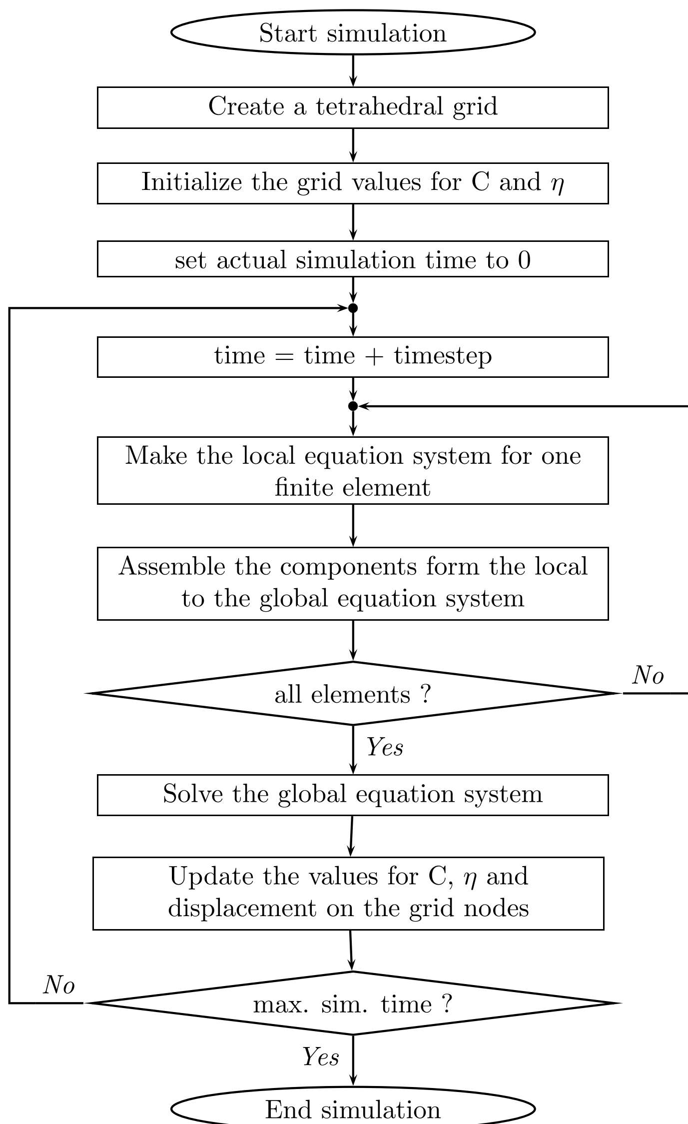

Fig. 1: Simulation procedure

As shown in Fig. 1, we iterate over all finite elements and build the local equation system for each element for every actual discrete time. The local equation system describes the oxidation process numerically for one element. In order to describe the oxidation process on the complete simulation domain we need a global coupled equation system. The components of the global equation system are assembled from the local equation system by using the superposition principle.

(c) 2005 The Electrochemical Society

After the iteration over all elements is finished, the global assembled equation system is also completed. Now the global non-linear equation system can be solved and we obtain the results for C, η, and the displacement values for the actual time step.

With these results we update the values for C, η, and the displacements on the grid nodes for the actual time step, such that these values are always keeping pace with the actual simulation time. The displacement vector enables the calculation of the strain tensor [19] as well as the stress tensor [7].

When the above described procedure is finished, we increase the actual simulation time and start with the assembling loop again. The same assembling and solving procedure is repeated for each time step until the desired end of the simulation.

REPRESENTATIVE EXAMPLES

First Example

We apply our oxidation model to the three-dimensional structure with (1.2×0.3) μm floor space, as displayed on Fig. 2. In this example the upper layer is a 0.15 μm thick Si_3Ni_4 - mask which prevents the oxidant diffusion on the subjacent Si - layer. Here the bottom surface is fixed and on the upper surface a free mechanical boundary condition is applied. The result of the oxidation process of the whole structure after a time t_1 is shown in Fig. 3.

For a more physical interpretation of the simulation results with a sharp interface between Si and SiO_2 the two regions can be extracted from the η - distribution by determining that $\eta \leq 0.5$ is SiO_2 and $\eta > 0.5$ is Si as shown in Fig. 4. For an optimal comparison of the geometry before and after oxidation as well as the influence of stress, Figs. 2 – 7 have the same perspectives and the same proportions.

Stress Dependence

In order to demonstrate the importance of the stress dependence we compare the results with and without the impact of stress. Since the oxidant diffusion and the chemical reaction are exponentially reduced with the hydrostatic pressure in the material, the oxidation process itself is highly stress dependent.

As shown in Fig. 5 the highest pressure in SiO_2 is under the edge of the Si_3Ni_4 - mask, because in this area the stiffness of the mask prevents the desired volume expansion of the newly formed SiO_2. Due to the mentioned stress dependence the oxidation rate in these areas is considerably reduced (see Fig. 4).

If the stress dependence is not included in the simulation of the oxidation process, the simulation results do not agree with the real physical behavior, because the oxidant diffusion and the chemical reaction also occur under the Si_3Ni_4 - mask without restriction. Because of this phenomenon the SiO_2 - region at the same oxidation conditions is much more expanded than with the stress dependence as shown in Fig. 6. In addition, the larger forces under the Si_3Ni_4 - mask, which result from the larger pressure domain (see Fig. 7) in this area, cause larger displacements of the mask.

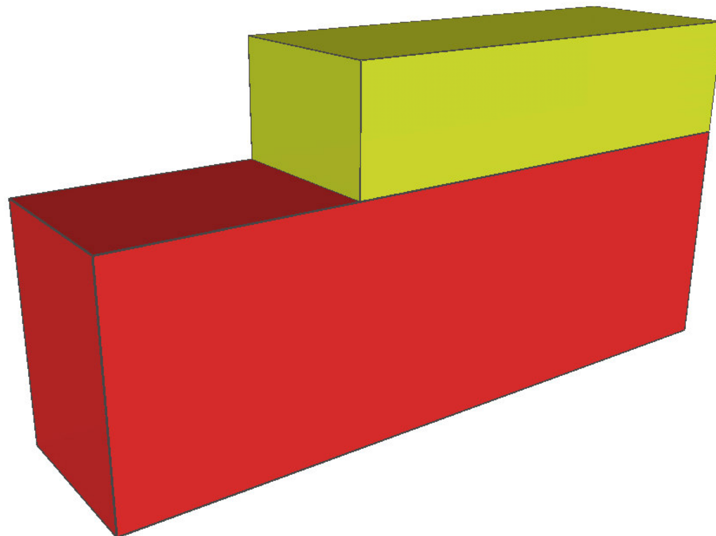

Fig. 2: Initial structure of the Si - Si_3Ni_4 - body before thermal oxidation

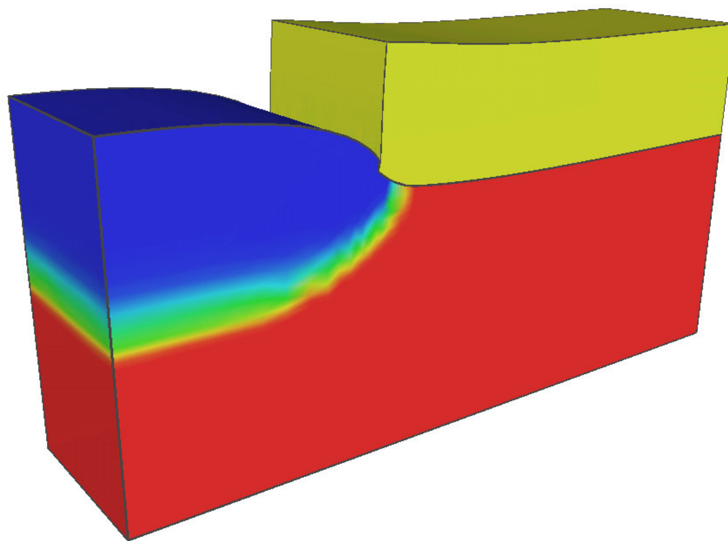

Fig. 3: η - distribution and reaction layer after thermal oxidation at time t_1

Second Example

Another more complex three-dimensional structure ((0.8 × 0.8) μm floor space), with a 0.15 μm thick L - shaped Si_3Ni_4 - mask is stress dependent oxidized with our oxidation model, as shown in Fig. 8. Due to the L - shaped mask here the effect of the three-dimensional oxidation process is pronounced, because the shape of the SiO_2 - region and the deformations are not continuous in any direction.

Fig. 9 shows that the highest pressure in SiO_2 is under the edge of the Si_3Ni_4 - mask again, which slows down the oxidation process in these areas. The stiffness of the Si_3Ni_4 - mask is approximately

(c) 2005 The Electrochemical Society

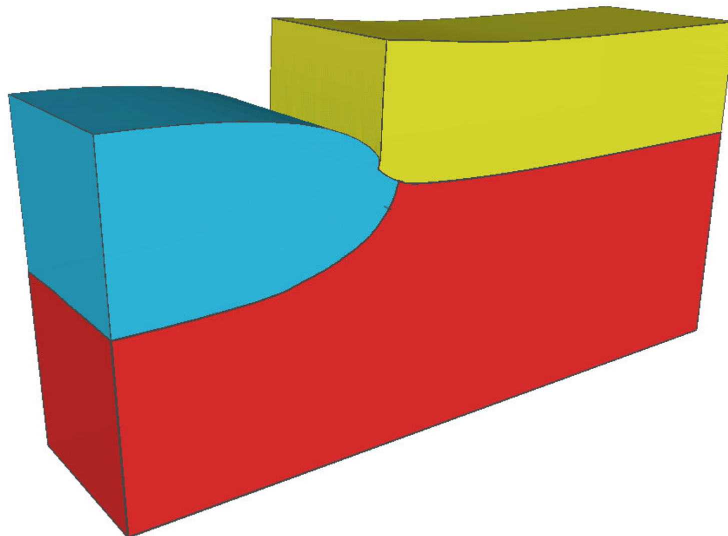

Fig. 4: SiO_2 - region (sharp interface) with stress dependent oxidation at time t_1.

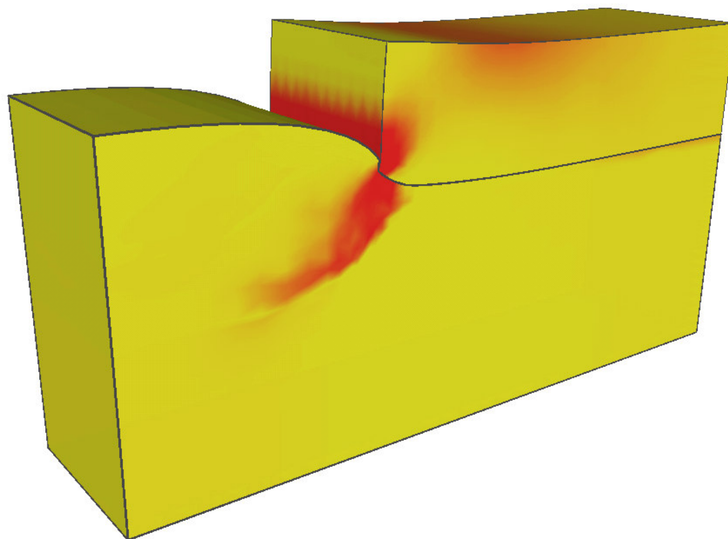

Fig. 5: Pressure distribution with stress dependent oxidation at time t_1.

six times larger than the stiffness of SiO_2 and so the displacements in SiO_2 are also much more larger than in the Si_3Ni_4 - mask which leads to the well-known bird's beak effect.

SUMMARY AND CONCLUSION

An oxidation model which takes the real physical behavior of the whole oxidation process under full control of the ambient parameters into account, has been presented. Our model is based on a normalized silicon concentration and a reaction layer with a spatial finite width in contrast to the moving boundary concept and a sharp Si - SiO_2 - interface in the conventional formulation.

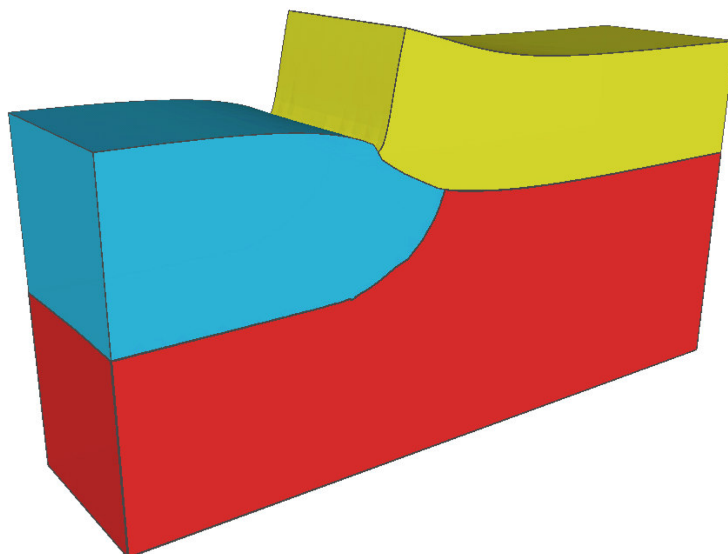

Fig. 6: SiO_2 - region (sharp interface) without stress dependent oxidation at time t_1.

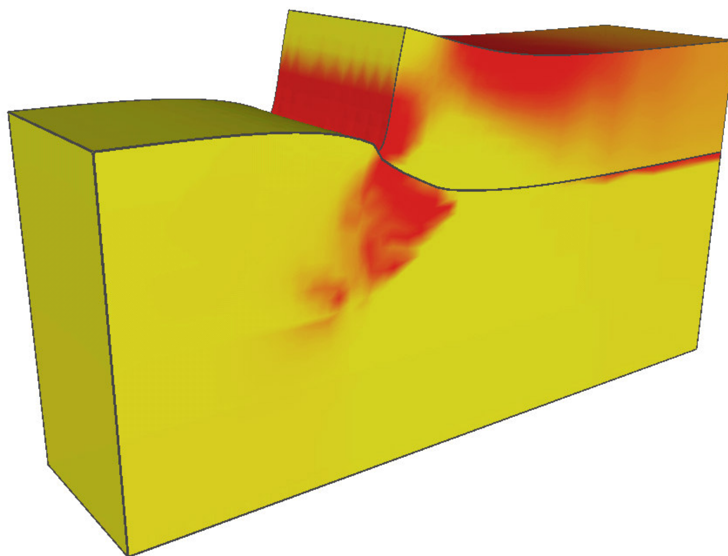

Fig. 7: Pressure distribution without stress dependent oxidation at time t_1.

The reaction layer takes into account that the diffusion of oxidants, the chemical reaction and the volume increase occur simultaneously. In contrast to the moving boundary concept, our normalized silicon concentration concept also works on complex three-dimensional structures without restriction. For a physical interpretation with a sharp interface between Si and SiO_2 the two regions can be extracted from the normalized silicon distribution by determining that a value equal or less 0.5 is SiO_2 and a value larger than 0.5 is Si. Furthermore thick film as well as thin film oxidation are properly treated without a need of modification.

For the mechanical behavior of the materials an elastic or viscoelastic model can be applied. In the viscoelastic model we use use a Maxwellian formulation. It was shown that for short time periods the Maxwell viscoelasticity can be expressed by an effective shear modulus which depends

(c) 2005 The Electrochemical Society

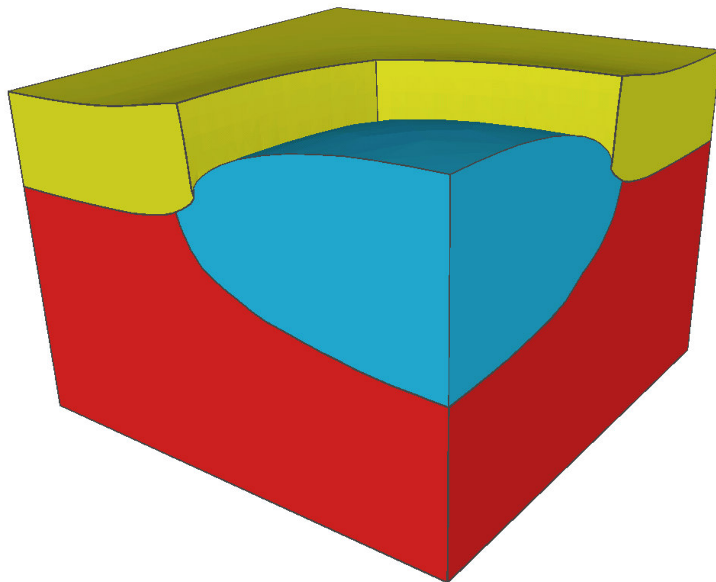

Fig. 8: SiO_2 - region with stress dependent oxidation at time t_1.

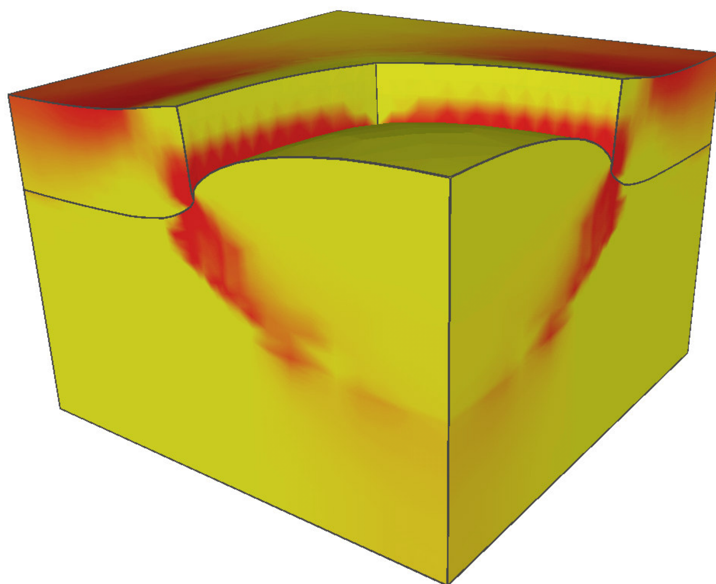

Fig. 9: Pressure distribution with stress dependent oxidation at time t_1.

on the Maxwellian relaxation time, in the deviatoric part of the so-called material matrix. The whole mathematical formulation of the oxidation process, which is described by a coupled system of partial differential equations, is solved by applying the finite element method.

The model was verified by the oxidation of two different three-dimensional structures. Beside the presentation of the simulation results the important influence of stress on thermal oxidation was investigated. It was shown that the highest hydrostatic pressure in SiO_2 is under the edge of the Si_3Ni_4 - mask and that the results agree only for stress dependent oxidation with the real

(c) 2005 The Electrochemical Society

physical behavior. As a result of the strong stress dependence of the oxidant diffusion and the chemical reaction the oxidation rate in this area is considerably reduced. If the stress is not taken into account the oxidation process also occurs under the Si_3Ni_4 - mask without restriction and so the SiO_2 - domain and the displacements are too large in relation to the real physical process.

REFERENCES

1. D. R. Hamann, *Phys. Rev. Lett.*, **81**(16), 3447 (1998).
2. Ch. Hollauer, H. Ceric, and S. Selberherr, in *Proc. 33rd European Solid - State Device Research Conference (ESSDERC 2003)*, p. 383, Estoril (2003).
3. E. Rank and U. Weinert, *IEEE Trans. on CAD*, **9**(5), 543 (1990).
4. B. E. Deal and A. S. Grove, *J. Appl. Phys.*, **36**(12), 3770 (1965).
5. A. Poncet, *IEEE Trans. on CAD*, **4**(1), 41 (1985).
6. S. Cea, PhD thesis, University of Florida, (1996).
7. V. Senez, S. Bozek, and B. Baccus, in *Proc. International Electron Devices Meeting (IEDM 1996)*, p. 705, San Francisco (1996).
8. H. Z. Massoud and J. D. Plummer, *J. Appl. Phys.*, **62**(8), 3416 (1987).
9. H. Z. Massoud, J. D. Plummer, and E. A. Irene, *J. Electrochem. Soc.*, **132**(7), 1746 (1985).
10. H. Z. Massoud, J. D. Plummer, and E. A. Irene, *J. Electrochem. Soc.*, **132**(11), 2685 (1985).
11. A. J. Moulson and J. P. Roberts, *Trans. Faraday Soc.*, **57**, 1208 (1961).
12. F. J. Norton, *Nature*, **191**, 701 (1961).
13. V. Senez et al., *IEEE Trans. on Elect. Dev.*, **43**(5), 720 (1996).
14. H. Matsumoto and M. Fukuma, in *Proc. International Electron Devices Meeting (IEDM 1983)*, p. 39, Washington (1983).
15. V. Senez et al., *J. Appl. Phys.*, **76**(6), 3285 (1994).
16. J. P. Peng, D. Chidambarrao, and G. R. Srinivasan, *COMPEL - The International Journal for Computation and Mathematics*, **10**(4), 341 (1991).
17. O. C. Zienkiewicz, *The Finite Element Method: Basic Formulation and Linear Problems*, McGraw-Hill, Maidenhead (1987).